Spatially Varying Elasticity in Image Registration

S. Kabus[1,2], A. Franz[2], and B. Fischer[1]
[1] Institute of Mathematics, University of Lübeck
[2] Philips Research Europe -- Hamburg, Sector Medical Imaging Systems

Correspondence to:
Sven Kabus
Philips Research Europe -- Hamburg
Röntgenstrasse 24-26
22335 Hamburg
Germany
Phone: +49 (0)40 5078 - 4562
Fax: +49 (0)40 5078 - 2510
E-mail: sven.kabus@philips.com

Summary

Objectives: In this paper we are concerned with elastic image registration. Usually, elastic approaches assume constant material parameters and result in a smooth displacement field. However, a constant choice has its shortcomings for images with varying elastic properties, like bones and soft tissue. The proposed method allows for spatially varying material properties.

Methods: The proposed variational registration scheme is based on a segmentation of the template image. Individual material properties can be assigned to each segmented region. The proposed variable elastic regulariser leads to a displacement field which is adapted to the locally chosen material properties.

Results: The capability of this approach is demonstrated by a synthetic and by real-life examples in two dimensions. For all examples the proposed method is compared to a conventional scheme where the material parameters are constants in the entire image domain.

Conclusions: A method for non-parametric registration which supports spatially varying elastic properties such as (in)compressibility or Young's modulus in certain image regions is proposed. It allows for registration results being more realistic compared to conventional approaches. Also, for a particular structure, an approximated preservation of volume or shape can be achieved.

Keywords

elastic image registration, variable regularisation, local material properties, volume preservation

1 Introduction

Nonrigid image registration is a challenging field of growing importance in medical imaging. The task is to find a vector field of displacements such that each point in a template image can be mapped onto a corresponding point in a reference image in a 'meaningful' manner.
By the notion 'meaningful' often a type of constraint is meant which prescribes identical elastic properties throughout the image domain. Typically, the displacement is computed subject to a smoothness constraint. A widely chosen constraint is realised by a regularisation based on the linear elastic potential of the displacement, see, e.g. [1] and references therein. Frequently, the constraint is applied globally with one global regularisation parameter and with elastic properties independent of the image position and, therefore, independent of the elastic behaviour of the corresponding anatomical structure.
Often, a globally uniform constraint provides satisfactory results due to the underlying physical model. Nevertheless, there exist several cases where anatomical structures behave different from each other. Soft tissue, for instance, is of different elasticity compared to bone structures. Therefore, the prescription of a uniform elastic behaviour may lead to deformations which are either unnecessarily restricted (when choosing elastic properties typical of bone structures) or physically unrealistic (if bone structures get deformed as soft tissue). Another demand for non-uniform behaviour occurs within the treatment evaluation of tumors. Here, preservation of shape or volume may be a reasonable property in a certain image region, i.e. the tumor region, but not in the entire image domain.
Therefore, in our view a 'meaningful' transformation supports local material properties as well as possibly approximates shape or volume preservation and requires, to this end, a spatially varying regularisation. As a consequence, further a priori knowledge has to be added.

In the literature one can find several attempts dealing with nonrigid image registration in conjunction with spatially varying regularisation or material parameters.
On the one hand, parametric approaches based on, for instance, damped spring models [2], radial basis functions [3], or B-splines with subsequent filtering [4] have been shown to allow for a locally varying deformability of the resulting displacement field. Although incorporating a kind of tissue constraint, these approaches tend to result in a displacement field interpolating smoothly across soft tissues, rather than to model the physics of tissue accurately. In particular, the elastic properties of tissue, such as its (in)compressibility or Young's modulus, cannot be controlled.
On the other hand, non-parametric approaches incorporating physical properties of tissue have been frequently proposed as part of a biomechanical model for brain applications. Here, based on a segmentation into (at least) bone and soft tissue structures, an initial estimate of the displacement field is computed. However, this estimate is restricted to the surfaces of the segmented regions. To model the displacement field in the entire domain, in a second step either the Navier-Lamé equations or the Navier-Stokes equations are employed. For the discretisation of the differential equations numerous

schemes are used, e.g. a finite difference method [5], a finite element method [6] or a boundary element method [7]. A related approach [8] is based on a finite element discretisation of the Navier-Lamé equations. Instead of using segmented surfaces as an initial estimate, a set of homologous landmarks (here provided by application of a snake algorithm to both images) is required to drive the deformation of the template image.
All these approaches have been reported to be accurate close to the segmented surfaces. However, since no volumetric information is exploited, the estimated displacement field may be less accurate far away from the surfaces.
The drawback of a possibly reduced accuracy can be overcome by including volumetric information [9-11]. These methods differ in the type of a priori information and underlying model. Whereas the a priori information is provided either by a segmentation of both images [10,11] or by statistical atlas information [9], the underlying model is based on the demons algorithm [10] or the Navier-Lamé equations [9,11].

The method presented in this note is based on a non-parametric registration scheme [1]. Regarding the interpretation of a meaningful transformation, the Navier-Lamé equations are employed as underlying model. Since these allow to model the elasticity of different anatomical structures, they are well suited to registration problems including both bone structures and soft tissue. Finally, we aimed at reducing the amount of a priori information as much as possible. Compared to previous work (e.g. [8,10,11]) where the a priori information was provided by segmentation of both images, here, a segmentation of the template image is sufficient.

The following section is concerned with the mathematical formulation of the registration problem whereas Section 3 reports on the application to a synthetic example as well as to real-life images.

2 Theory and Methodology

Let $T, R : \Omega \rightarrow G$ denote the template and the reference image, respectively. Here, *G* denotes a set of grey values and, for simplicity, $\Omega \subseteq \Re^2$ the image region. In addition, let a meaningful segmentation of T be given. That is, a decomposition of Ω into disjoint regions Ω_l is assumed, such that Ω is equal to the union of all regions.
The registration aims at finding a displacement field $u : \Omega \rightarrow \Re^2$ such that $T_u := T(id + u)$ is similar to R, where id denotes the identity mapping. In mathematical terms, the similarity is described by a functional $D[u; T, R]$. It can be chosen as any popular distance (or similarity) measure provided its Gâteaux derivative exists. However, this note is restricted to the common sum of squared differences,

$$D[u; T, R] = \int_{\Omega} [R(x) - T_u(x)]^2 \, dx =: \int_{\Omega} L^D \, dx , \tag{1}$$

which assumes monomodal images.

A registration based on a similarity measure only, may yield a deformed template image which perfectly matches the reference image as long as all grey values are present in both images. However, the problem is ill-posed [1] and the underlying deformation does in general not make sense in a physical context. Therefore, an additional smoothness constraint (or regulariser) is considered which can be chosen to model the application specific physical properties. In this note we investigate a regulariser based on the popular linear elastic potential which is in addition equipped with spatially varying Lamé parameters λ, μ (the so-called *variable elastic regulariser*),

$$S[u; \lambda, \mu] = \frac{1}{4} \int_{\Omega} \mu_u \sum_{i,j=1}^{2} \left(\partial_{x_j} u_i + \partial_{x_i} u_j \right)^2 + 2\lambda_u (\nabla \cdot u)^2 \, dx =: \int_{\Omega} L^S \, dx \,, \tag{2}$$

where λ_u and μ_u are defined in analogy with T_u, e.g. $\lambda_u := \lambda(id + u)$. For other regularisers including diffusive-, fluidal- or curvature-based approaches we refer to, e.g., [1]. Generally, a regulariser may be interpreted as a penaliser: According to the underlying physical model, it is designed to keep the displacement field smooth during deformation.
In contrast to a conventional approach, where λ and μ are global constants, both parameters are assumed to be spatially dependent. Here, the positive functions $\lambda, \mu : \Omega \to \Re^+$ are used to reflect the material properties. They can be related to the possibly more familiar Young's modulus and Poisson's ratio: From a qualitative point of view, μ is inversely proportional to the elastic modulus and λ / μ is proportional to the incompressibility of the material. In [8] it is reported that for the same type of anatomical structure the values used in the literature differ a lot. Consequently, a choice of material parameters in a relative way rather than in an absolute one is suggested.
By knowing the segmentation of the template image we are now in a position to assign dedicated elastic properties to each subdomain Ω_l. Thereby diverse elastic behaviour of different materials, like bones and muscles, can be simulated.
Note, that λ_u and μ_u depend on the displacement u. This dependency is indispensable due to the fact that nonlinear registration approaches mostly employ an iterative scheme and therefore the material properties at a fixed position do change in the course of the registration. As a consequence, the parameters at an intermediate stage can be deduced from u applied to the initial setting which makes a segmentation of the reference image redundant.

By combining the similarity measure and the regularising term, the problem is to find a displacement field u which minimises the joint functional

$$J[u] := D[u] + S[u] = \int_{\Omega} L^D dx + \int_{\Omega} L^S dx \,. \tag{3}$$

Usually, the regularising term is weighted by an additional regularisation parameter [1] which is chosen with regard to the application dependent smoothness of the resulting displacement field. Here, the weighting of the regularising term is based on the Lamé parameters only and the additional parameter is omitted.
The computation of the Gâteaux derivative of (3) yields a necessary condition for a minimiser of (3),

$$\nabla_u L^D + \nabla_u L^S - \nabla_{\nabla u} L^S = 0 \,,$$

where ∇_u refers to the gradient with respect to u whereas $\nabla_{\nabla u}$ denotes the gradient with respect to the Jacobian of u.
The outcome is a system of nonlinear partial differential equations equipped with associated boundary conditions,

$$\begin{aligned} Au(x) - f(u) &= 0, \quad x \in \Omega, \\ \frac{\partial u_i(x)}{\partial n} &= 0, \quad x \in \partial\Omega, i = 1,2. \end{aligned} \tag{4}$$

For the similarity measure and the variable elastic regulariser a straightforward calculation yields

$$\begin{aligned} Au :=& -\nabla \cdot \left[\mu_u \left(\nabla u + \nabla^T u\right)\right] - \nabla \left[\lambda_u \nabla \cdot u\right] \\ &+ \frac{1}{4} \sum_{i,j=1}^{2} \left(\partial_{x_j} u_i + \partial_{x_i} u_j\right)^2 \nabla \mu_u + \frac{1}{2} \left(\nabla \cdot u\right)^2 \nabla \lambda_u, \\ f(u) :=& \left(R - T_u\right) \nabla T_u. \end{aligned} \tag{5}$$

Note that $Au = f(u)$ corresponds to the Navier-Lamé equations. The boundary conditions in (4) are of Neumann type but clearly they may be chosen problem dependent.
For a numerical treatment, (4) is embedded into an initial boundary value problem followed by a discretisation using second order finite differences as described in [12].
From a mathematical point of view, the scheme can be easily extended to three dimensions. However, from a computational point of view, an extension to three dimensions requires more care. Whereas for the conventional approach, where the Lamé parameters are constant, a fast solution scheme is available [1], it cannot be transferred to the proposed approach.

3 Results

The proposed method has been applied to both synthetic and medical images in two dimensions. Here, we present two examples. At first, an elastic phantom is considered, where the aim is to define a parameter setting which can be used in medical applications. At second, slices from MR data sets are registered.

The elastic phantom (Fig. 1, top left) consists of two objects: a square object representing some soft tissue and in its inside a circle object taking the role of, for instance, a tumor. For the transition from the template to the reference image (Fig. 1, bottom left) we model a shrinkage of the tissue object. Due to the invisibility of the circle object in the reference image a conventional registration approach will tend to shrink its size in order to relate it as much as possible to a circle of zero size.
The variable elastic regulariser has been employed with three different parameter settings. For the first setting, the Lamé parameters are constant ($\lambda \equiv 0.01, \mu \equiv 0.4$), cf. the second column of Fig. 1. For the second and the third setting μ (cf. third column) and λ (cf. last column) are multiplied by 1000, respectively. Here, the aim is to compare the conventional case with settings preserving either shape or volume of a certain image region.

The resulting deformation fields have been compared with respect to the deformed template image and the displacement field (top row in Fig. 1) and the quantity $|1 + \nabla u|$ (bottom row). Here, a volume preserved region (corresponding to $|1 + \nabla u| = 1$) is depicted by medium grey, whereas a contracting (expanding) region appears in light grey (dark grey).
With no further material knowledge we observe in the second column a shrinkage of the tumor object (reduction in volume is 30%), indicated by a light grey of the circle object in the volume map. With a large μ or λ either a shape (and volume) preservation (third column) or an approximated volume preservation only (last column) can be seen. For both cases the change in volume is less than 0.3%.

As the medical example an application concerning the assessment of the kinematic motion of joints has been investigated. Template and reference image show sagittal slices from an MR exposure of a human knee at different degrees of flection. A series of such images is typically given in kinematic imaging [13]. Firstly, every pair of subsequent images is registered from which a mapping between any two images can be deduced. Secondly, in one image a number of positions is chosen by a physician such that, based on the mappings, the other images can be automatically aligned according to the one selected.
Here, we investigate the first step which is the key part and determine a displacement field for each subsequent pair of a series consisting of five images (cf. Fig. 2, top centre, for a depiction of the first two images). For each transition from template onto reference image we expect a displacement field with the largest deformation in the region corresponding to the knee joint. In contrast, in the regions corresponding to femur and tibia, a rigid transformation is a reasonable assumption.
Each pair of images is registered using the common elastic matching scheme with no spatially varying parameters and the proposed method based on a manual segmentation of femur, tibia, and femorotibial articulation in the template image (shown top right). For all experiments, the parameter setting was $\lambda \equiv 0, \mu \equiv 0.025$ for the common elastic scheme while values of $\lambda \equiv 0$, $\mu(x) = 25$ and $\mu(x) = 0.005$ are employed in the regions of femur/tibia and femorotibial articulation, respectively. For the purposes of stability and computational effort, a multi-resolution pyramid with four levels is used in all cases.
For the first image pair, results are shown in the bottom row of Fig. 2 with a zooming on the bone area. The two images on the left-hand side correspond to the constant setting whereas the two images on the right depict the results for the varying setting. A comparison of the resulting deformations reveals no visible improvement for the deformed templates (first and third image) at a first glance. However, when filling the regions corresponding to femur and tibia (retrospectively the registration) with a chequerboard pattern, a non-rigid deformation of both regions becomes visible (second image in bottom row). Moreover, the shape of the femur near to the femorotibial articulation is deformed. This is caused by a structure included in the reference image but not in the template image leading to a downward movement of the femur. Such a failure of registration does not happen for the second experiment.

Here, the bone structures are rigidly displaced and the result is not misled in the region of the femorotibial articulation (bottom right). For a quantitative evaluation of the displacement fields according to the bone structures, we inserted each related displacement field into a thin-plate spline and computed its bending energy as described by [14]. Here, a bending energy of zero is expected for a rigidly deformed object whereas its evaluation for a non-rigid deformation returns a positive value. Table 1 displays the normalised energy values with respect to femur and tibia for all the eight experiments. In each case we observe for the proposed method a reduction of energy to about 1% when compared to the common elastic scheme.

All experiments have been computed on a standard PC. The Matlab-implementation takes about 10 minutes for an image of size 256x256.

4 Conclusion and Discussion

In this work, a scheme for image registration has been derived which allows for spatial variation of elastic properties. Possible medical applications include intrapatient applications such as kinematic motion of joints as well as follow-up studies.
Based on a segmentation of the template image, individual elastic properties can be assigned to dedicated anatomical structures. The underlying physical model in conjunction with spatially varying material properties allows not only for prescribing an individual elastic behaviour but also for approximating a preservation of shape or volume in a certain image region. However, exact values for the material parameters are not known in general and, usually, are guessed for in vivo situations. Work is in progress to evaluate various parameter settings as being typical for specific applications.
Compared to previous results, now, the segmentation of the template image only is sufficient. This is an important issue for time-critical tasks, like brain-shift, since an (often time-consuming) segmentation is required for the pre-operatively generated image only.
As a necessary condition for a clinical use of the proposed scheme, a fast implementation for three dimensions is required. For the conventional case, where the material parameters are constants, a numerical scheme to solve the arising system of linear equations with linear-logarithmic complexity is described in the literature [1]. Although the structure of the system coincides with the one in the case of variable parameters, the numerical scheme cannot be used for the proposed method. Instead, a multigrid scheme appears as an appropriate alternative. Beside from the numerical complexity, the storage amount is an important issue. Here, a fast implementation is required to avoid the additional storage of parameter maps (having the same size as the images) as well as, for a given image position, a costly computation of material parameters from the segmentation.

References

1. Modersitzki J. Numerical methods for image registration. Oxford: Oxford University Press; 2004.
2. Edwards PJ, Hill DLG, Little JA, Hawkes DJ. A three-component deformation model for image guided surgery. Medical Image Analysis. 1998:2(4):355-67.
3. Duay V, D'Haese P-F, Li R, Dawant BM. Non-rigid registration algorithm with spatially varying stiffness properties. In: IEEE International Symposium on Biomedical Imaging: ISBI. 2004; Arlington, USA. IEEE; 2004. p. 408-11.
4. Staring M, Klein S, Pluim J. Nonrigid registration with adaptive, content-based filtering of the deformation field. In: Fitzpatrick JM, Reinhardt JM, editors. Medical Imaging 2005: Image Processing. Proceedings of the SPIE; 2005; San Diego, USA. SPIE; 2005. p. 212-21.
5. Davatzikos C. Nonlinear registration of brain images using deformable models. In: Proceedings of the IEEE Workshop on Mathematical Methods in Biomedical Image Analysis (MMBIA '96); 1996; San Francisco, USA. IEEE; 1996. p. 94-103.
6. Ferrant M, Nabavi A, Jolesz FA, Kikinis R, Warfield SK. Registration of 3-d intraoperative MR images of the brain using a finite-element biomechanical model. IEEE Transactions on Medical Imaging. 2001:20(12):1384-97.
7. Ecabert O, Butz T, Nabavi A, Thiran JP. Brain shift correction based on a boundary element biomechanical model with different material properties. In: Ellis RE, Peters TM, editors. Medical Image Computing and Computer-Assisted Intervention – MICCAI 2003, Proceedings of the 6th International Conference; 2003; Montreal, Canada. Berlin: Springer; 2003. p. 41-49.
8. Hagemann A, Rohr K, Stiehl HS, Spetzger U, Gilsbach JM. Biomechanical modeling of the human head for physically-based, non-rigid image registration. IEEE Transactions on Medical Imaging. 1999:18(10): 875-84.
9. Rexilius J, Handels H, Nabavi A, Kikinis R, Warfield SK. Automatic nonrigid registration for tracking brain shift during neurosurgery. In: Meiler M, Saupe D, Kruggel F, Handels H, Lehmann T, editors. Bildverarbeitung für die Medizin 2002, Algorithmen – Systeme – Anwendungen. BVM 2002: Proceedings des Workshops; 2002; Leipzig, Germany. Berlin: Springer; 2002. p. 135-38.
10. Ehrhardt J, Handels H, Strathmann B, Malina T, Plötz W, Pöppl SJ. Atlas-based recognition of anatomical structures and landmarks to support the virtual three-dimensional planning of hip operations. In: Ellis RE, Peters TM, editors. Medical Image Computing and Computer-Assisted Intervention – MICCAI 2003, Proceedings of the 6th International Conference; 2003; Montreal, Canada. Berlin: Springer; 2003. p. 17-24.
11. Kabus S, Franz A, Fischer B. On elastic image registration with varying material parameters. In: Meinzer H-P, Handels H, Horsch A, Tolxdorff T, editors. Bildverarbeitung für die Medizin 2005, Algorithmen – Systeme – Anwendungen. BVM 2005: Proceedings des Workshops; 2005; Heidelberg, Germany. Berlin: Springer; 2005. p. 330-34.
12. Kabus S, Franz A, Fischer B. Variational image registration with local properties. In: Pluim JPW, Likar B, Gerritsen FA, editors. Biomedical Image Registration. WBIR 2006: Proceedings of the Third International Workshop; 2006; Utrecht, The Netherlands. Berlin: Springer; 2006. p. 92-100.
13. Bystrov D, Pekar V, Meetz K, Schulz H, Netsch T. Motion compensation and plane tracking for kinematic MR-imaging. In: Liu Y, Jiang T, Zhang C, editors. Computer Vision for Biomedical Image Applications. CVBIA 2005: Proceedings of the First International Workshop; 2005; Beijing, China. Berlin: Springer; 2005. p. 551-60.
14. Bookstein FL. Principal Warps: Thin-Plate Splines and the Decomposition of Deformations. IEEE Transactions on Pattern Analysis and Machine Intelligence. 1989:11(6): 567-85.

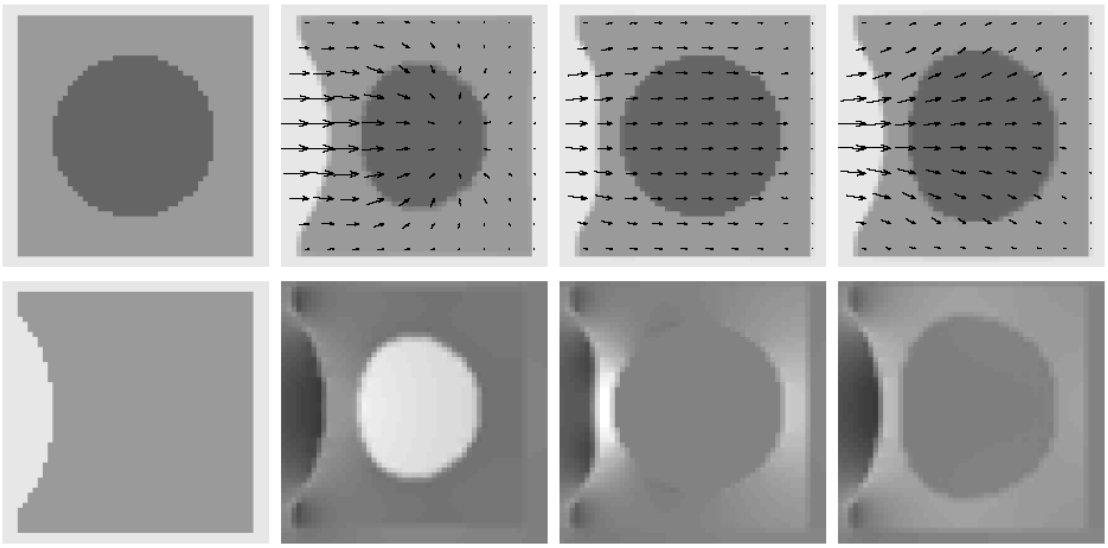

Figure 1: The left column shows template (top) and reference image (bottom). Beside, the results from three different settings are depicted columnwise: in the top row with respect to the deformed template and overlayed with the displacement field (data are thinned out for better recognition) and in the bottom row with respect to the volume preservation indicator, cf. text for further details.

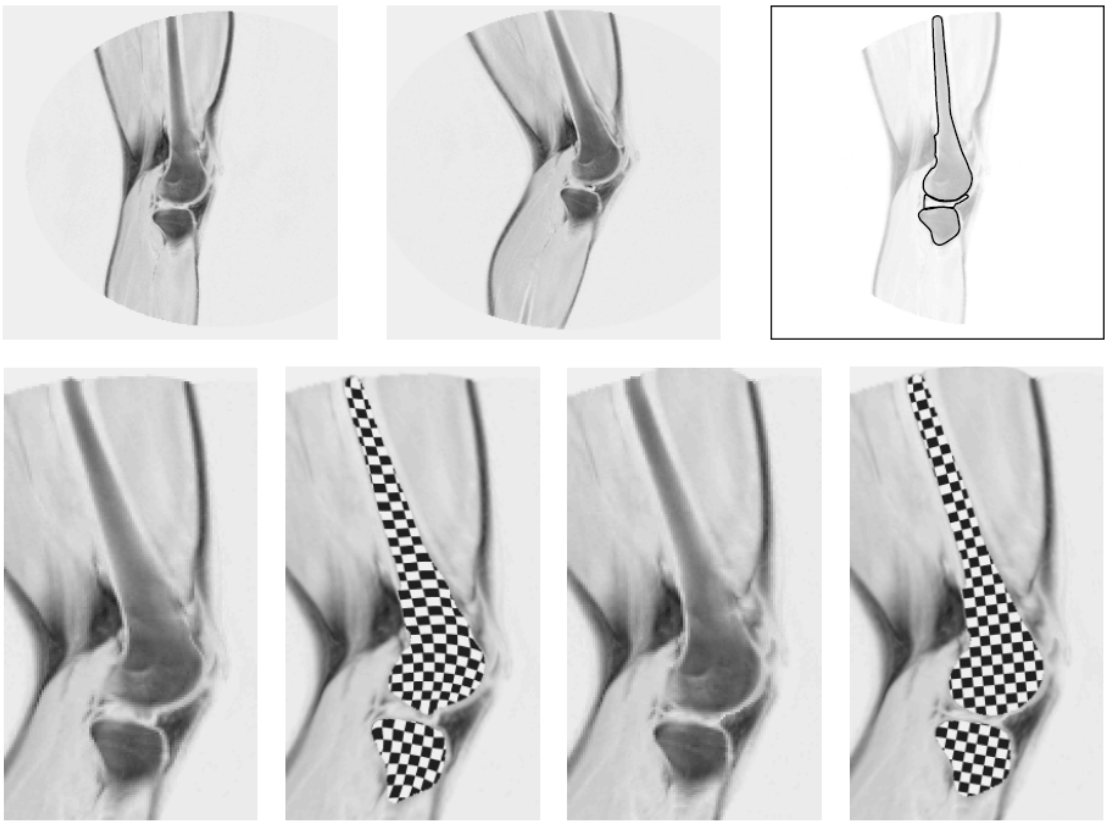

Figure 2: Template, reference, and segmented template image are shown in the top row from left to right (the grey-values are inverted for better recognition). Below, zooms into the deformed template are depicted. The first two images correspond to the case with constant parameters ($\lambda \equiv 0, \mu \equiv 0.025$), the last two images result from the case with variable parameters ($\mu(x) = 25$ and $\mu(x) = 0.005$ in the regions of tibia/femur and femorotibial articulation, respectively, as well as $\lambda(x) = 0$ everywhere). See text for further details.

image pair to be registered	common elastic scheme		proposed method	
	femur	tibia	femur	tibia
1 to 2	106.239	187.701	1.500	1.051
2 to 3	86.270	95.616	1.113	1.050
3 to 4	66.420	68.382	0.860	0.386
4 to 5	56.144	92.586	0.797	0.688

Table 1: Normalised bending energies with respect to the displacement fields within femur and tibia.